THE Hg REGION: SUPERDEFORMATION AND OTHER SHAPES

R. V. F. Janssens[a], M. P. Carpenter[a], M. W. Drigert[b], P. B. Fernandez[a], E. F. Moore[a], D. Ye[c], I. Ahmad[a], K. B. Beard[c], I. Bearden[d], Ph. Benet[d], P. J. Daly[d], U. Garg[c], Z. W. Grabowski[d], T. L. Khoo[a], W. Reviol[c] and F. L. H. Wolfs[a]

a: Argonne National Laboratory, Argonne, IL 60439, USA
b: Idaho National Engineering Laboratory, Idaho Falls, ID 83415, USA
c: University of Notre Dame, Notre Dame, IN 46556, USA
d: Purdue University, West Lafayette, IN 47907, USA

1. INTRODUCTION

First experimental evidence for a new region of superdeformation near A~190 is only about one year old: a band of 12 transitions with an average energy spacing of 37 keV, an average dynamic moment of inertia $\mathcal{J}^{(2)}$ of 110 $\hbar^2$MeV^{-1} and an average quadrupole moment of 18 $\pm$ 3 eb was observed in ^{191}Hg[1]. This result confirmed predictions[2-5] from a variety of theoretical approaches for the occurrence of superdeformed nuclei in this region with a major to minor axis ratio of 1.65:1 (β~0.5). Several important questions were raised by the original experimental result. First, the dynamic moment of inertia $\mathcal{J}^{(2)}$ was found to increase steadily with rotational frequency $\hbar\omega$. Mean-field calculations which attempt to reproduce the variation in $\mathcal{J}^{(2)}$ have suggested that such a rise may be attributed to three major factors which could contribute separately or cooperatively: (i) shape changes as a function of $\hbar\omega$ (centrifugal stretching), (ii) changes in pairing at large deformations[6] and (iii) occupation of specific high-j orbitals[6,7] ($i_{13/2}$ protons and $j_{15/2}$ neutrons). Questions regarding (i) the existence of other SD nuclei in this region and (ii) the limits in N and Z of the SD regions also needed attention.

In the past year, an impressive number of new results have become available; some of these will be reviewed in this contribution and in the presentation by R. M. Diamond. In fact, all the SD bands known in this region are given in Fig. 1, with the exception of SD structures in ^{194,195}Tl, which have been reported at this conference for the

first time by R. M. Diamond. Here, we shall first summarize the present experimental situation concerning ^{192}Hg, the nucleus regarded as the analog of ^{152}Dy[8] for this SD region in that shell gaps are calculated[5] to occur at large deformation for Z=80 and N=112. Proton and neutron excitations out of the ^{192}Hg core will then be reviewed with particular emphasis on ^{191}Hg and ^{193}Tl. The implications of the results for pairing at large deformations and the need to consider other degrees of freedom (such as octupole correlations) will be addressed. The presentation will conclude with a brief discussion on other shapes seen in this region, with a particular emphasis on ^{191}Hg.

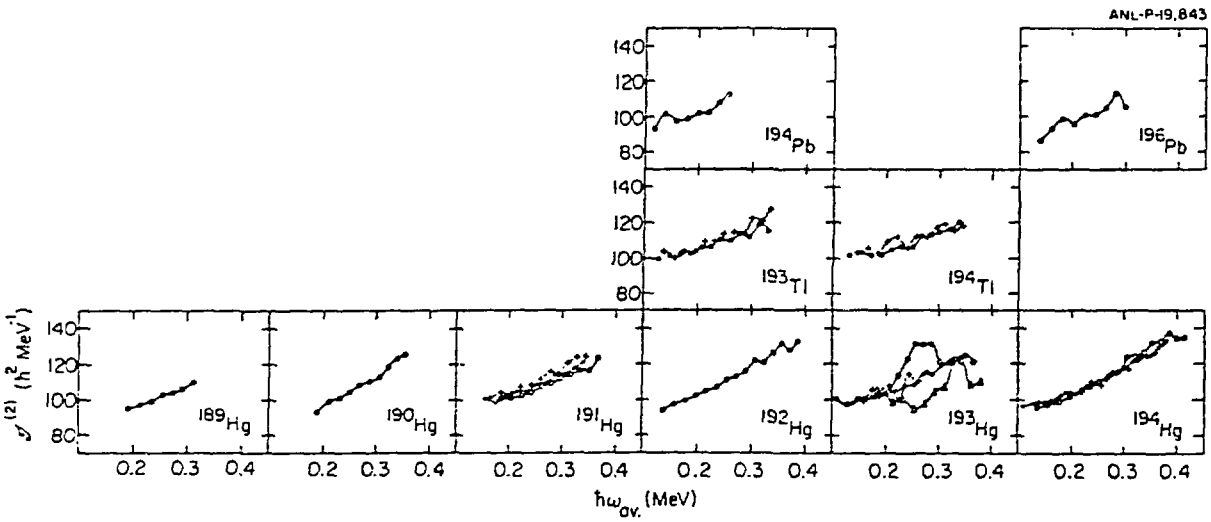

Fig. 1. Summary of the known SD bands in the A~190 region (from Ref. 22).

2. SUPERDEFORMATION IN ^{192}Hg

The SD band of ^{192}Hg as measured at ATLAS with the ^{160}Gd(^{36}S,4n) reaction at 162 MeV[9] is presented in Fig. 2. This band has also been observed in an independent experiment by Becker et al.[10], and the results are in good agreement. A band of 16 transitions extending in energy from 257 to 792 keV was observed. From Fig. 2 it is clear that the band feeds the known levels up to 8^+ in the positive-parity yrast sequence and up to 9^- in the negative parity band. Transitions which link the superdeformed band with known yrast levels could not be found. It is likely that many different decay paths share the

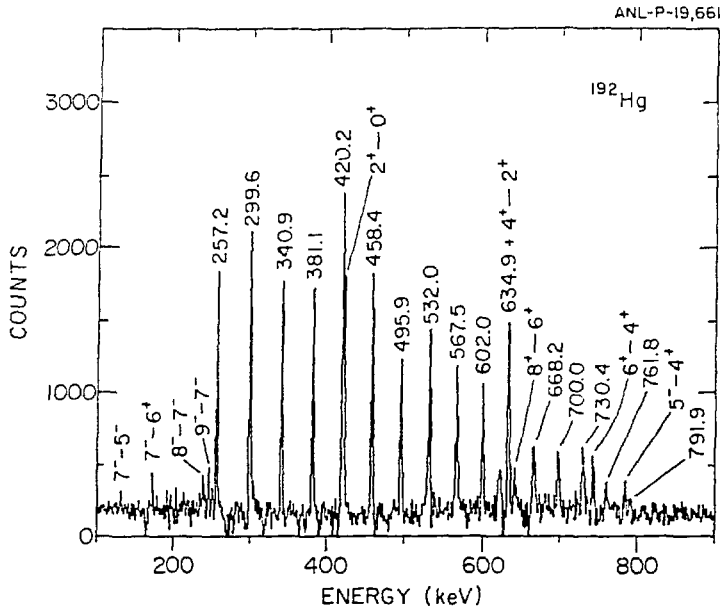

Fig. 2. Superdeformed band in ^{192}Hg (from Ref. 9).

intensity and that the link is statistical in nature. This assumption is supported by the observation that the feeding into the yrast states is spread over several states belonging to two bands of opposite parity. The average entry spin into the yrast states is ~8ħ. The spin of the lowest level in the SD band (fed by the 257-keV γ-ray) was estimated to be 10ħ from the the deexcitation pattern out of the superdeformed band, the average entry spin into the yrast states and the assumption of a $\Delta\ell=2\hbar$ angular momentum removal by the transitions linking the SD states and the yrast line[9]. The same spin value is also obtained in Ref. 10 from a procedure where $J^{(2)}$ is fit by a power series expansion in ω^2, which is then integrated to give the spin. The highest spin observed is then most probably 42ħ. With these assumed spin values, a static moment of inertia $J^{(1)}$ can be derived: the latter is presented as a function of $\hbar\omega$ together with the values of $J^{(2)}$ in Fig. 3. It is striking that (1) there is a large monotonic increase (40%) in $J^{(2)}$ with $\hbar\omega$, (2) the $J^{(2)}$ values for ^{192}Hg are similar, but always higher than those for ^{191}Hg at the same frequency (Fig. 32), and (3) $J^{(2)}$ is significantly larger than $J^{(1)}$ for all values of $\hbar\omega$. All of these observations are a challenge for theory to explain.

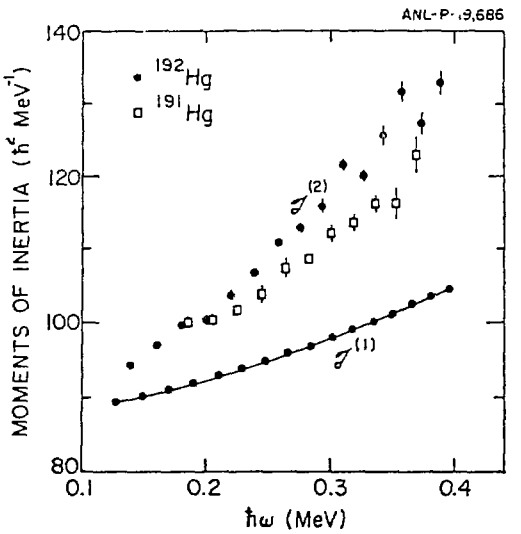

Fig. 3. Static and dynamic moments of inertia $\mathcal{J}^{(1)}$ and $\mathcal{J}^{(2)}$ for ^{192}Hg. $\mathcal{J}^{(2)}$ for ^{191}Hg is given for comparison.

Lifetimes within the SD band in ^{192}Hg were measured with the Doppler-shift attenuation method (DSAM)[11]. In contrast with previous measurements, where only fractional Doppler shifts $F(\tau)$ are reported[1,8], we have been able to analyze detailed lineshapes for individual transitions between SD states ($\beta_2 \sim 0.5$). Analysis of individual lineshapes allows one to determine the variation of Q_t as a function of $\hbar\omega$, as opposed to previous studies where Q_t was assumed to be constant for all states in the band. In addition, information is also obtained on the feeding times into the SD structure. The measurement was performed with the reaction mentioned above at the beam energy of 159 MeV. The target was a 1 mg/cm^2 isotopically enriched foil on which 14 mg/cm^2 Au had been evaporated. An analysis in terms of broadened lineshapes was possible for transitions with $458 \leq E_\gamma \leq 700$ keV. In order to extract lifetimes from these broadened lineshapes, the computer code LILIFI[12] was used. Details of the analysis can be found in Ref. 11.

The lifetimes were transformed into transition quadrupole moments $Q_t(I) = (1.22 \langle I020/I-2 \rangle^2 \tau E_\gamma^5)^{-1/2}$ assuming the spin values given above. The Q_t-values are displayed as a function of $\hbar\omega$ in Fig. 4b. As can be

seen, the quadrupole moment Q_t, and hence the deformation, remain essentially constant over the entire frequency range. This result rules out centrifugal stretching as an explanation for the rise in $J^{(2)}$: this is illustrated by the dashed line in Fig. 4b where the values of Q_t have been derived assuming that the change in $J^{(2)}$ is entirely due to a variation in deformation. As already discussed by Ye et al.[9], mean-field calculations without pairing, such as those by Chasman[5] or Åberg[13], give proton and neutron contributions to $J^{(2)}$ which remain essentially constant with $\hbar\omega$. Thus, the increase in $J^{(2)}$ cannot be accounted for by the occupation of specific high-j orbitals: this points to the need to examine the effects of pairing.

In order to interpret the results presented above, cranked shell model calculations with pairing (CSM) were performed using a Woods-Saxon potential. The approach is similar to the one described in detail in Ref. 6, 14 and 15. In the discussion below, use is also made of the neutron and proton single-particle routhian diagrams in Ref. 14. These calculations reveal a pronounced proton gap at Z=80 which remains open for all frequencies considered. The resulting proton configuration contains four N=6 ($i_{13/2}$) protons ($\pi 6^4$). For the neutron system, single-particle gaps exist at N=112 and N=116, lying between the second and the third N=7 ($j_{15/2}$) orbitals with Ω=3/2 and 5/2, respectively. The gaps are separated by the two deformation-aligned levels [512]5/2 and [624]9/2. Very similar single-particle level diagrams have been obtained in the Woods-Saxon model of Ref. 5. The resulting neutron configuration contains four $j_{15/2}$ neutrons and, thus, the SD configuration in ^{192}Hg can be labelled ($\pi 6^4 \nu 7^4$). Figure 4a compares the calculated dynamic moment of inertia with the data. In the calculation, pairing correlations were treated self-consistently by means of the particle number projection procedure[6]. The rise in the calculated $J^{(2)}$ can be ascribed to the combined gradual alignment of a pair of N=6 ($i_{13/2}$) protons and of a pair of N=7 ($j_{15/2}$) neutrons within the frequency range under consideration. The evolution of the nuclear shape with $\hbar\omega$ was also calculated[11]. The inset in Fig. 4b illustrates that within the frequency range of interest the predicted changes in β_2 and β_4 are very small. The

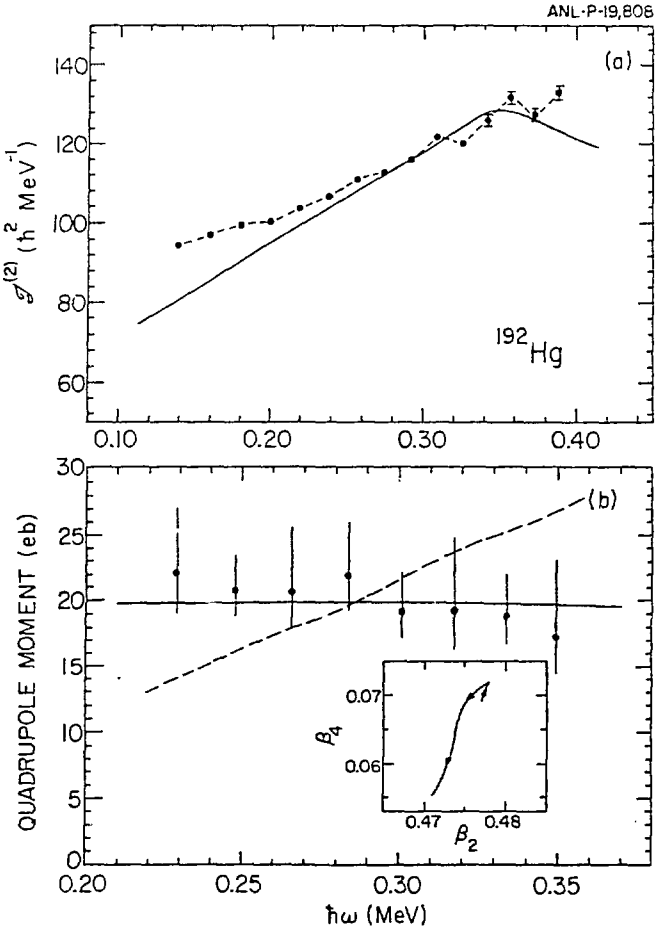

Fig. 4a) Comparison between the measured and calculated dynamic moment of inertia for ^{192}Hg.

b) Comparison between the measured and calculated Q_t values in the SD band of ^{192}Hg. The dashed curve is a calculation assuming that the rise in $\mathcal{J}^{(2)}$ is due to a change in deformation only, the solid line is a cranked shell model calculation. The inset shows the calculated change in deformation parameters β_2 and β_4 over the frequency range of interest.

resulting Q_t-values agree well with the measured values as is shown by the solid line in Fig. 4b. The success of the calculations in reproducing all aspects of the data allows us to propose that quasiparticle alignments and the resulting changes in pairing represent a major factor contributing to the rise in $\mathcal{J}^{(2)}$ in ^{192}Hg and, probably, in other nuclei in this region. Further evidence for this conclusion is discussed below.

3. NEUTRON AND PROTON EXCITATIONS: THE CASE OF ^{191}Hg AND ^{193}Tl

We have shown in section 2 that the data for the "doubly magic" SD nucleus ^{192}Hg can be described successfully in cranking calculations using a Woods-Saxon potential. The same calculations can also be tested in neighboring nuclei and specific predictions are available[14]. Detailed spectroscopy in the SD minimum has revealed multiple band structures in ^{194}Hg, ^{193}Hg and ^{191}Hg (Refs. 14-16,19). First, we shall compare experiment with calculations in ^{191}Hg. Figure 5 presents spectra for the two new SD bands (bands 2 and 3) in this

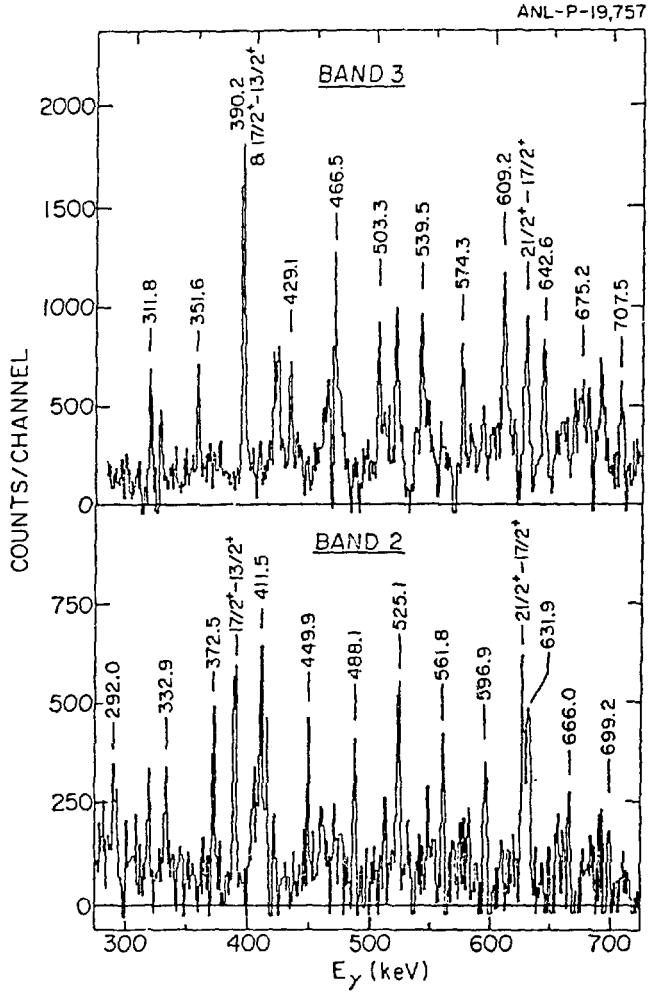

Fig. 5. Excited superdeformed bands in ^{191}Hg (from Ref. 15).

nucleus. Each band corresponds to ~0.8% of the events in ^{191}Hg (as measured with the ^{160}Gd(^{36}S,5n) reaction at 172 MeV; the SD band reported earlier[1] (band 1) has a corresponding intensity of 2%). The three bands have essentially the same intensity pattern, i.e. the intensity remains constant in the frequency range $0.175<\hbar\omega<0.24$ MeV and decreases gradually at higher rotational frequencies. The decay out of bands 2 and 3 occurs at lower frequency than in band 1 with the γ-ray intensity decreasing gradually below $\hbar\omega$=0.175 MeV. Information on the lifetimes of the states was obtained for a few of the new transitions from a thick target experiment with the Doppler-shift attenuation method (see Refs. 1, 15 for details): the deformation in the bands was found to be very similar.

Figure 6a presents the dynamic moments of inertia for the 3 bands as a function of $\hbar\omega$. In all cases, $\mathcal{J}^{(2)}$ is again seen to increase with $\hbar\omega$. Furthermore, the average values of $\mathcal{J}^{(2)}$ for bands 2 and 3 (110 and 113 $\hbar^2$MeV^{-1}, respectively) are somewhat larger than the corresponding value for band 1 (108 $\hbar^2$MeV^{-1}) and are close to the value reported for ^{192}Hg (113 $\hbar^2$MeV^{-1}). For γ-ray energies below 400 keV, the transition energies of band 3 are almost exactly intermediate to the energies of band 2: the situation is similar to that reported[14] for ^{194}Hg where the two excited bands exhibit the same feature over a larger energy range. In analogy with Ref. 14, bands 2 and 3 are interpreted as "signature partners". The degree of signature splitting can then be inferred from Fig. 6b where the experimental single-particle routhians e' for bands 2 and 3 are presented as a function of $\hbar\omega$. These routhians were calculated under the assumption that the bands are strongly coupled at low $\hbar\omega$. The excitation energies were arbitrarily taken as 4.5 MeV and 4.64 MeV for bands 2 and 3, respectively, and the spins were estimated with the method proposed in Ref. 10. We note that the spins derived in this way, i.e. 25/2 and 27/2 for the bandheads of bands 2 and 3, respectively, differ by one unit and are consistent with the strong coupling picture presented here. The energy of the core was approximated by a Harris parametrization from fits to the low levels of the known yrast SD bands in ^{192}Hg and ^{194}Hg. It can be seen from

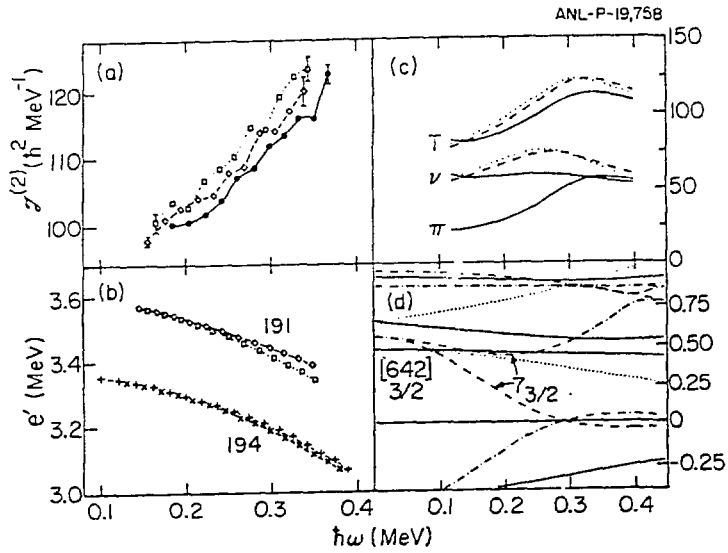

Fig. 6. Experimental (a) and calculated (c) dynamic moments of inertia for the three SD bands in ^{191}Hg. Experimental single-particle routhians for the excited SD bands in ^{191}Hg and ^{194}Hg (b) and quasiparticle routhians for N=111 (d) (see Ref. 15 for details).

Fig. 6b that, with the assumptions outlined above, the two bands may be proposed as signature partners for $\hbar\omega$<0.2 MeV (i.e. they follow the same smooth trajectory) and exhibit increasing signature splitting for $\hbar\omega$>0.2 MeV. This behavior differs from that observed[14] in ^{194}Hg (shown for comparison in Fig. 6b): in this case the two excited bands show very little signature splitting over the entire frequency range.

The results can be compared with the cranked shell model calculations described above. Figure 6d presents the neutron quasiparticle routhians for ^{191}Hg. The yrast SD configuration is built on the aligned $\nu 7_{3/2}$ routhian with parity and signature quantum numbers (π=-,r=+i). We associate this configuration with band 1. Bands 2 and 3 can be understood as the signature partners built on the [642]3/2 orbital with quantum numbers (π=+,r=+i) and (π=+,r=-i), respectively. The evolution of the calculated $\mathcal{J}^{(2)}$ values for the 3 bands as a function of $\hbar\omega$ is given in Fig. 6c where the individual contributions of the proton and neutron configurations under discussion are also presented. The major contribution to the rise of $\mathcal{J}^{(2)}$ in the three bands is caused by the gradual alignment of the $\pi 6^4$

protons. The neutron contributions differ for band 1 and bands 2 and 3. In band 1, the N=7 neutron crossing is blocked whereas it is present in bands 2 and 3. As a consequence, the neutron contribution to $J^{(2)}$ remains almost constant for band 1 while an additional increase is calculated for bands 2 and 3. The calculations reproduce the data rather well for $\hbar\omega \geq 0.2$ MeV as can be seen from a comparison between Fig. 4a and 4c. As discussed in Ref. 6, the larger deviations between theory and experiment at lower frequencies can be attributed to the renormalization procedure used in the calculations. The signature partner of band 1 (π=-,r=-i) is calculated to lie several hundred keV higher in excitation energy because of the large signature splitting (Fig. 6d) and, as a result, the corresponding rotational band should be more difficult to observe experimentally. The calculated values of $J^{(2)}$ in bands 2 and 3 are similar to that of the lowest SD band in ^{192}Hg since all three have the same content in intruder orbitals (four N=6 ($i_{13/2}$) protons and four N=7 ($j_{15/2}$) neutrons). Furthermore, it is seen in Fig. 6d that the ν[642]3/2 routhians form a coupled structure below $\hbar\omega \sim 0.15$ MeV, while signature splitting increases gradually at higher frequencies. In the calculations without pairing, this signature splitting is present as well, although slightly reduced[14]. These features are present in the data and can be considered as strong arguments in favor of the assignments presented here. It should, however, be mentioned that another possible assignment for bands 2 and 3 could involve the neutron orbitals [512]5/2 and [624]9/2 mentioned above. This possibility cannot be excluded a priori as the calculations are expected to reproduce the positions of the single-particle states to within a few hundred keV only. However, these orbitals are calculated to remain strongly coupled over the entire range in $\hbar\omega$ and no significant signature splitting would result. This is contrary to the experimental observations and reinforces our assignment based on the ν[642]3/2 orbital for this SD nucleus.

An equally successful description in terms of the cranked shell model has been presented for ^{194}Hg in Ref. 14. In this nucleus, 3 SD bands have been observed in separate experiments at Daresbury[14] and at

Berkeley[16]. The lowest neutron excitations are predicted to involve transitions from the [512]5/2 to the [624]9/2 Nilsson level. This leads to pairs of strongly coupled bands showing no signature splitting. Bands 2 and 3 in this nucleus are interpreted as a signature partner pair since the γ-ray energies of band 3 are observed to lie mid-way between those of band 2 to within 1 keV and both bands are of similar intensity.

We have recently completed a study[17] of ^{193}Tl which has one proton outside the Z=80, N=112 core. This nucleus was produced under similar conditions (angular momentum input and excitation energy) as all the nuclei discussed above with the reaction ^{160}Gd(^{37}Cl,4n)^{193}Tl at 167 MeV. Two SD bands of 13 transitions each were found (see Fig. 7). The total γ-ray flux through the two bands is about equal and corresponds at most to 0.5% (per band) of all decays in ^{193}Tl. Because of the weak population, information on the decay towards the known yrast states is rather fragmentary and judged insufficient to propose spins on the basis of the observed feeding pattern into the yrast line. We note that the two bands persist to frequencies somewhat lower than those seen in ^{192}Hg and comparable to those reported[14,16] for ^{194}Hg. Figure 8a presents the dynamic moments of inertia $J^{(2)}$ for the two bands as a function of $\hbar\omega$ and also provides a comparison with ^{192}Hg. Again, $J^{(2)}$ increases with $\hbar\omega$ for both bands even though the rise occurs mainly for $\hbar\omega$>0.2 MeV: the situation has some resemblance to that observed in band 1 of ^{191}Hg where $J^{(2)}$ is also flat at the lowest frequencies. From Fig. 7, it can also be seen that for the two bands the transition energies are almost intermediate to one another, at least up to an energy of 400 keV. As in the case of bands 2 and 3 of ^{191}Hg, we present experimental single-particle routhians e' as a function of $\hbar\omega$ in Fig. 8b. The computation of these routhians was also performed assuming excitation energies of 4.5 and 4.61 MeV for the bands 1 and 2, respectively. The spins were estimated with the method of Ref. 10 and found to be 19/2 and 21/2 at the bottom of the two bands. A Harris parametrization to the levels of the SD band in ^{192}Hg was used to obtain the energy of the rotating core. All the evidence strongly suggests that the two bands can be considered as signature partners.

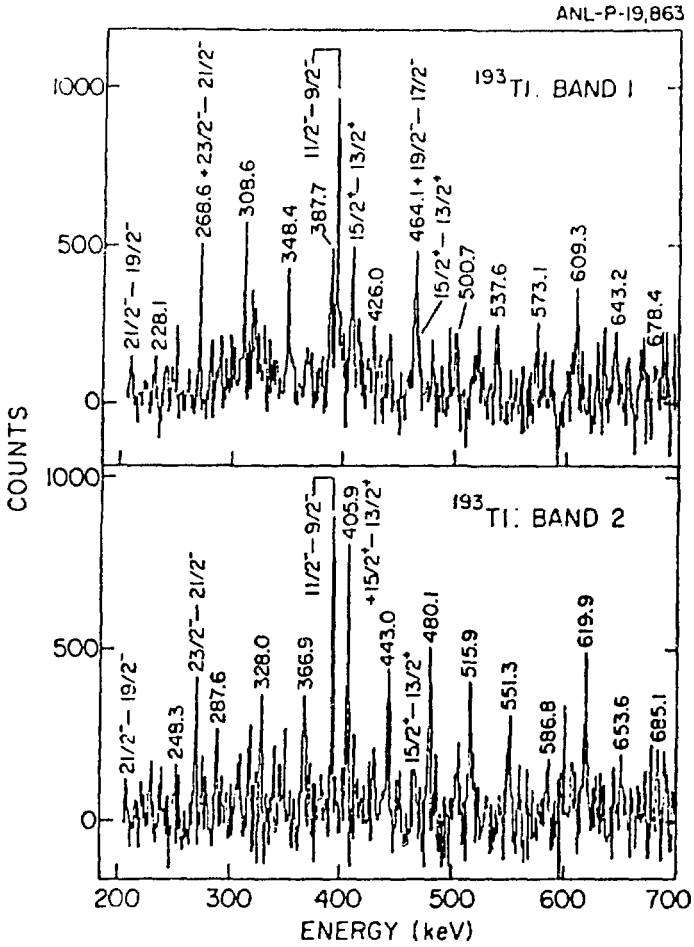

Fig. 7. Superdeformed bands in ^{193}Tl (from Ref. 17).

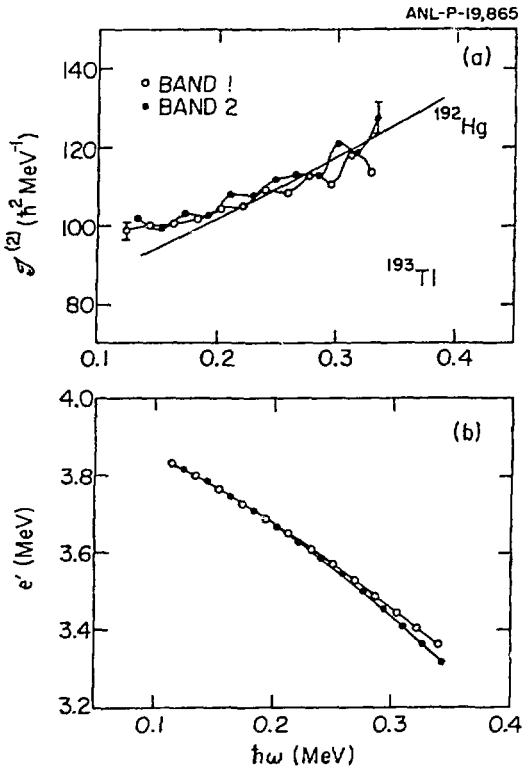

Fig. 8a) Dynamic moments of inertia for the SD bands in ^{193}Tl. ^{192}Hg is given for comparison.

b) Experimental routhians for the SD bands in ^{193}Tl.

At the lowest frequencies the bands are strongly coupled while splitting increases gradually above $\hbar\omega$=0.2 MeV.

The results can again be interpreted very nicely within the cranked shell model calculations with pairing. Above the Z=80 gap lies the third $i_{13/2}$ proton orbital with Ω=5/2. The fact that the third $i_{13/2}$ orbital is populated will result in an increase in the value of $\mathcal{J}^{(2)}$ with respect to ^{192}Hg at the lowest frequencies as observed experimentally. At low frequency, the two signature partners for this orbital are degenerate and a strongly coupled structure is expected. Splitting is calculated to occur at frequencies $\hbar\omega$>0.2 MeV, as seen experimentally.

From the discussion above it can be concluded that a good description of the SD bands can be achieved. Two points need, however, to be reemphasized:

-(i) the inclusion of pairing is crucial for reproducing the data and, in particular, the smooth increase of $\mathcal{J}^{(2)}$ with $\hbar\omega$. The pairing correlations are calculated to be rather weak and are therefore mainly of dynamical character. In the proton system, pairing is reduced by the presence of the Z=80 closure. As was shown in Refs. 9 and 14, the calculations require that the neutron pairing be reduced as well if one wants to reproduce the similarities in the behavior of $\mathcal{J}^{(2)}$ with $\hbar\omega$ observed in <u>all</u> nuclei in this region.

-(ii) as pointed out in Ref. 18, the transition energies in some of the SD bands are very close to SD bands in neighboring nuclei (for example, transitions in bands 2 and 3 in ^{191}Hg are within 1 to 2 keV of transitions in bands of ^{193}Hg) and all bands can be related to ^{192}Hg. These similarities have been linked to intrinsic spin alignments and underlying symmetries which are discussed by R. M. Diamond in his presentation.

Finally, one should also come back to the case of ^{193}Hg where 4 SD bands have been observed by Cullen et al.[19]. As can be seen from Fig. 1, two of these bands have strikingly different dynamical moments of inertia from all previously observed SD bands in this region, i.e. one shows a strong upbend at the frequency where the other shows a strong downbend. These two bands cannot be accounted for satisfactorily in

the CSM calculations discussed above. A possible clue for an explanation comes from the experimental evidence for E1 transitions between one of the two irregular bands and the yrast SD band. This, together with the reduced alignments observed and the strong interaction between crossing bands, is interpreted as evidence for strong octupole correlations in this nucleus at large deformations. Clearly, more data will be needed to confirm this explanation.

4. OTHER NUCLEAR SHAPES IN ^{191}Hg

Since this conference is also dedicated to gamma-soft nuclei it is certainly worthwhile to discuss briefly the wealth of information that is becoming available on the yrast structure of nuclei in this region. Here, we focus on the case of ^{191}Hg, the nucleus studied in the greatest detail. In addition to the 3 SD bands, a total of 14 different band structures has been established in ^{191}Hg (Ref. 20,21). Most of the latter are rotational bands exhibiting band crossings with various degrees of alignment which represent excellent tests of CSM calculations for oblate, collective nuclei ($\beta_2 \sim 0.2$, $\gamma \sim -60°$). A detailed comparison between the data and the CSM results can be found in Ref. 20. Here we focus our attention to a particular level sequence presented in Fig. 9. For spins lower than 41/2, all band structures show the regular level patterns with connecting E2 transitions characteristic of collective rotation. Above the 41/2 level on the other hand, the transition energies vary greatly and a large number of dipole and quadrupole transitions compete in the decay. This feature together with the fact that the band decays toward several rotational structures indicates that the new levels differ greatly in character from the rotational yrast states at lower excitation energy. These properties are very similar to those observed in nuclei near A~150. In these cases, the angular momentum is generated by the alignment of the spins of individual nucleons along the symmetry axis and the overall nuclear shape resulting from this particle-alignment mode is oblate. On the basis of this similarity, it is proposed that the new level structure in ^{191}Hg is also of single-particle character and is associated with a non-

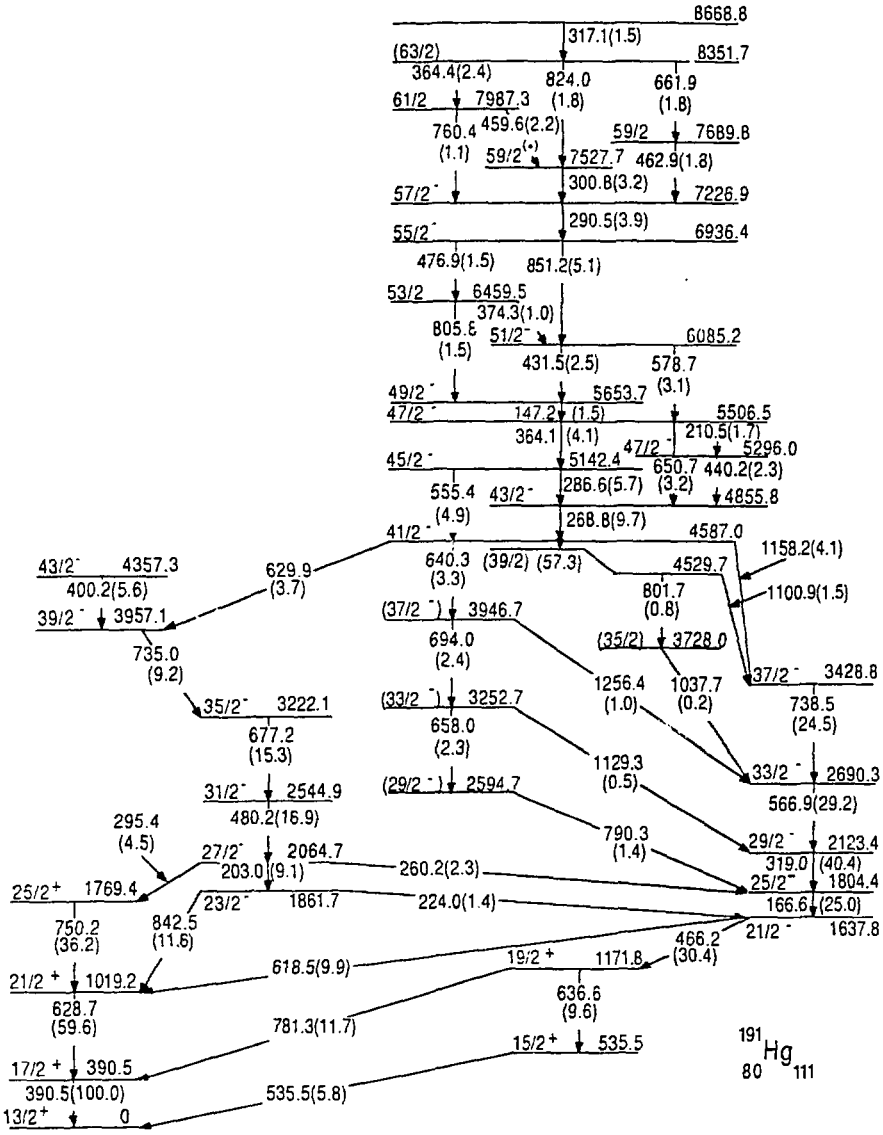

Fig. 9. Partial level scheme of ^{191}Hg showing the new level structure discussed here. See Ref. 21 for detail.

collective prolate shape (β_2~0.15, γ=-120°). Nilsson-Strutinsky calculations support this assignment[21]. They show that the driving force towards γ=-120° is provided by the presence of several quasi-holes in high-j orbitals in the same way as quasiparticles in high-j shells drive the neutron deficient A~150 nuclei towards oblate non-collective rotation. This makes the ^{191}Hg nucleus a good example for a rich variety of phenomena indicative of different nuclear shapes (oblate-collective, superdeformed and prolate non-collective), and analogies can be drawn with the rich level structure of ^{152}Dy.

5. CONCLUSIONS

During the past year, considerable knowledge has been gained on superdeformation in the A~190 region. In fact, superdeformation is now known to occur in at least eleven nuclei in this region. From the data discussed here, it was possible to rule out centrifugal stretching as the cause for the rise in $\mathcal{J}^{(2)}$ with $\hbar\omega$. Consecutive alignment of $\nu j_{15/2}$ and $\pi i_{13/2}$ orbitals seems to provide a consistent explanation. The inclusion of pairing for reproducing the $\mathcal{J}^{(2)}$ behavior is crucial even though there is evidence that the pairing correlations are rather weak. These conclusions were obtained within the framework of the cranked shell model. It is, however, also realized that the model has its limitations. The contribution by R. M. Diamonds emphasizes the close correlation between the transition energies in many bands and those in the SD band of ^{192}Hg which strongly suggest the occurrence of intrinsic spin alignments reflecting an underlying symmetry in the SD nuclei. The possibility that octupole correlations play an important role was also discussed. Finally, we have briefly indicated that evidence exists for other nuclear shapes.

ACKNOWLEDGEMENT

The authors express their deep gratitude to R. Chasman, W. Nazarewicz, M. Riley, F. S. Stephens, R. M. Diamond and R. Wyss for many stimulating discussions and S. Pilotte and F. Scarlassara for assistance in the ^{193}Tl experiment. This work was supported in part by the Department of Energy, Nuclear Physics Division, under contracts nos W-31-109-ENG-38, DE-AC07-76ID01570 and DE-FG02-87ER40346, by the National Science Foundation under grant PHY88-02279.

REFERENCES

1) Moore, E. F. et al., Phys. Rev. Lett. 63, 360 (1989).
2) Tsang, C. F. and Nilsson, S. G., Nucl. Phys. A140, 275 (1970).
3) Caillian, M., et al., Phys. Lett. 46B, 11 (1973).
4) Bengtsson, T. and Ragnarsson, I., Nucl. Phys. A436, 14 (1985).
5) Chasman, R. R., Phys. Lett. 219B, 227 (1989).

6) Nazarewicz, W. et al., Phys. Lett. 225B, 208 (1989), and Nucl. Phys. A503, 285 (1989).
7) Bengtsson, T. Ragnarsson, I. and Åberg, S., Phys. Lett. 208B, 39 (1988).
8) Nolan, P. J. and Twin, P. J., Ann. Rev. Nucl. Part. Science 38, 533 (1988).
9) Ye, D. et al., Phys. Rev. C41, R13 (1990).
10) Becker, J. et al., Phys. Rev. C41, R9 (1990).
11) Moore, E. F. et al., Phys. Rev. Lett. 64, 3127 (1990).
12) Emling, H. et al., Phys. Lett. 217B, 33 (1989).
13) Åberg, S., Phys. Scr. 25, 23 (1982).
14) Riley, M. A. et al., Nucl. Phys. A512, 178 (1990).
15) Carpenter, M. P. et al., Phys. Lett. 240B, 44 (1990).
16) Beausang, C. W. et al., Z. Physik A335, 325 (1990).
17) Fernandez, P. B. et al., Nucl. Phys. in print.
18) Stephens, F. S. et al., Phys. Rev. Lett. 65, 301 (1990).
19) Cullen, D. M. et al., Phys. Rev. Lett. 65, 1546 (1990).
20) Ye, D. et al., to be published.
21) Ye, D. et al.; Phys. Lett. 236B, 7 (1990).
22) Janssens, R. V. F. et al., Nucl. Phys. in print.